

## NANOPARTICLE CHARACTERISTICS AFFECTING ENVIRONMENTAL FATE AND TRANSPORT THROUGH SOIL

THOMAS K. DARLINGTON, ARIANNE M. NEIGH,\* MATTHEW T. SPENCER, OANH T. NGUYEN, and STEVEN J. OLDENBURG  
nanoComposix, 4878 Ronson Court, Suite K, San Diego, California 92111, USA

(Received 21 July 2008; Accepted 28 December 2008)

**Abstract**—Nanoparticles are being used in broad range of applications; therefore, these materials probably will enter the environment during their life cycle. The objective of the present study is to identify changes in properties of nanoparticles released into the environment with a case study on aluminum nanoparticles. Aluminum nanoparticles commonly are used in energetic formulations and may be released into the environment during their handling and use. To evaluate the transport of aluminum nanoparticles, it is necessary not only to understand the properties of the aluminum in its initial state but also to determine how the nanoparticle properties will change when exposed to relevant environmental conditions. Transport measurements were conducted with a soil-column system that delivers a constant upflow of a suspension of nanoparticles to a soil column and monitors the concentration, size, agglomeration state, and charge of the particles in the eluent. The type of solution and surface functionalization had a marked effect on the charge, stability, and agglomeration state of the nanoparticles, which in turn impacted transport through the receiving matrix. Transport also is dependent on the size of the nanoparticles, although it is the agglomerate size, not the primary size, that is correlated with transportability. Electrostatically induced binding events of positively charged aluminum nanoparticles to the soil matrix were greater than those for negatively charged aluminum nanoparticles. Many factors influence the transport of nanoparticles in the environment, but size, charge, and agglomeration rate of nanoparticles in the transport medium are predictive of nanoparticle mobility in soil.

**Keywords**—Nanomaterials Aluminum Surface charge Particle size Characterization

## INTRODUCTION

The production and use of engineered nanomaterials is increasing exponentially, and inevitably, significant quantities of nanomaterials will be released into the environment. The desirable properties of nanoparticles are related to their dimensions; however, evidence suggests that the toxicity of nanoparticles may be much greater than the toxicity of bulk formulations with the same chemistry [1–4]. One of the challenges for determining the risk associated with a nanomaterial release event is the uncertainty regarding how the properties of nanomaterials change once they interact with the environment as well as how the weathered conditions of the nanomaterials affect where and how the nanoparticles are distributed and in what condition they may contact biota [5,6] (<http://www.raeng.org.uk>).

Extensive characterization of the nanomaterials before, during, and after experiments is necessary to interpret transport data and to generate accurate risk assessments [7–10]. Particle size, size distribution, shape, surface and core chemistry, agglomeration state, crystallinity, redox potential, purity, catalytic activity, surface charge, and porosity are all important in understanding nanoparticle behavior [3,4,10–12]. In addition, the nanoparticle characteristics are affected by experimental conditions, such as soil chemistry, pH, and organic matter content. Properties considered to be particularly relevant for characterizing transport in soils are the size and surface state of the nanomaterials when suspended in different solution environments [13,14]. For example, the majority of nanoparticles

will agglomerate in biologically relevant fluids, and the increase in particle size affects the transportability and toxicity of the formulation [12,15]. In addition, different preparation methods can affect experimental results. Carbon fullerenes produced by extended mixing in water had differing surface properties, shape, and agglomerate size compared with fullerenes created by a solvent exchange process [16].

The potential for changes in nanoparticle properties with exposure to environmental conditions and the impact on transport are illustrated through a case study on aluminum nanoparticles. Aluminum was selected because it currently is used at the nanoscale in a number of applications, including energetics, alloys, coatings, incendiary devices, and sensors [17]. Nanoscale metals, including aluminum, in combination with metal oxides, are attractive for use as energetics because of their high energy release on oxidation. Reduction in the size of aluminum particles from 3,000 to 30 nm reduces the ignition time and doubles the burn rate of energetic formulations [18]. The increase in reaction rate is related most closely to the specific surface area of the aluminum, which increases by orders of magnitude when particle sizes are reduced from the micron- to the nanoscale. Because of the nature of the aluminum nanoparticle applications, the potential for aerosolization of aluminum nanoparticles and subsequent deposition of the nanoparticles across large areas, particularly at military proving grounds, is high. Currently, the U.S. Air Force is testing devices containing aluminum nanoparticles at sites in northwestern Florida (USA) that include diverse flora and fauna. Understanding the fate and transport of nanoparticles is critical to ensure that the impact of nanoparticles released to the environment is minimized. Evaluation of aluminum nano-

\* To whom correspondence may be addressed  
([arianne.neigh@nanocomposix.com](mailto:arianne.neigh@nanocomposix.com)).  
Published on the Web 1/28/2009.

particle properties both before and after environmental exposure is necessary for determining the appropriate mitigation steps after a release event.

A definitive need exists to evaluate the effects that nanoparticles may have on the environment, yet little is known regarding interactions of nanoparticles with environmental matrices, either naturally or in the test environment. Ecotoxicity literature has focused on *in vitro* or *in vivo* studies of nanoparticles in aquatic systems [4,19], but to date, few studies have identified toxicity in terrestrial species [20–22] or focused on transport in a terrestrial environment with an aim of providing data relevant for prediction of nanoparticle behavior and evaluation of exposure pathways [23]. Nanoparticle transport experiments have been focused primarily on maximizing delivery of zero-valent metals to soil and groundwater for remediation purposes [24,25]; however, because nanoscale aluminum generally is not of interest for remediation, little data are available regarding its transport in soils. To our knowledge, Doshi et al. [26] is the only other study that evaluated transport of nanoaluminum. Transport through porous sand media was observed for both 100 nm oxide-coated and carboxylated aluminum, and transport varied with surface coating and pH of the suspension solutions. The present study focuses on high-level characterization of the nanoaluminum in suspension and in the soil matrix to gain a better understanding of the properties that affect transport. In addition, we evaluate particles in different environmentally relevant suspensions, aluminum particles of different sizes, and transport through two different types of soil.

## MATERIALS AND METHODS

### *Nanoparticle preparation*

Aluminum nanoparticle powder was purchased from Novacentrix™ with nominal diameters of 50, 80, and 120 nm and a 1- to 2.5-nm aluminum oxide passivation layer, as reported by the manufacturer. Primary particle diameters were calculated based on transmission-electron microscopy (TEM; JEM-1010; Jeol) and image-processing software (ImageJ; National Institute of Mental Health). Particle statistics and distributions were calculated using Microsoft Excel and SYSTAT® software (Systat Software). Because particles were approximately spherical, axes of individual particles were randomly measured for sizing purposes. Basic statistics for particle diameters and particle distribution histograms were calculated by TEM and based on the percentage of total particles measured, percentage of total mass, and percentage of total surface area. Outliers in data measurements beyond three-fold the interquartile range were excluded from evaluation of average particle size but were included in describing the range of the data. Two outliers and one outlier were excluded for the 80- and 120-nm particles, respectively. Particle diameters were log-transformed to obtain a normal distribution, with the geometric mean and 95% confidence interval of particle diameters reported on the back-transformed data.

Two different experimental designs were evaluated, top-loaded columns and suspension-loaded columns, with different preparations of starting materials. The top-loaded columns mimicked leaching of nanoparticles with water infiltration in terrestrial environments via a spill or aerosol deposition. Top-loaded columns used the powdered starting material (8–10 mg) with no additional preparation. The suspension-loaded columns mimicked dispersion in a high-shear environment followed by release, which constitutes a worst-case scenario of

Table 1. Properties of solutions for aluminum suspensions at 25°C in Milli-Q® water (Milli-Q), moderately hard reconstituted water (MHRW), and a phosphate solution

Media	pH	Total hardness (mg/L as CaCO <sub>3</sub> )	Alkalinity (mg/L as CaCO <sub>3</sub> )
Milli-Q water	5.5	0	0
MHRW	7.7	90	64
3.4 mM phosphate	6.7	0	77

environmental exposure. Particles used for the suspension-loaded experiments were prepared in room-temperature degassed Milli-Q® water (Milli-Q), 3.4 mM phosphate buffer (monosodium and disodium phosphate; pH 6.6), or moderately hard reconstituted water (MHRW) [27] by probe sonication (30 pulses for 1 s/cycle at 50% output; W-380 sonicator, CL4 375-W converter head; Heat Systems Ultrasonics) at a concentration of 1,000 mg/L. Particles suspended in phosphate are referred to hereafter as treated particles, whereas particles in MHRW or water are referred to as untreated particles. Treated and untreated suspensions were immediately diluted in water or MHRW to 50 mg/L. Particles were prepared 15 min before introduction to the soil column. Alkalinity, hardness, and pH of suspension solutions before adding the aluminum nanoparticles are reported in Table 1. Samples were monitored using ultraviolet–visible light spectroscopy (HP 8453 Ultraviolet-Visible Spectrophotometer, Hewlett Packard), laser Doppler electrophoresis, and dynamic light scattering (Malvern Zetasizer Nano ZS). Surface charge is reported as the zeta potential. The hydrodynamic diameter is reported as the intensity-weighted *Z* average, with the polydispersity index width representing the standard deviation about the *Z* average assuming a monomodal distribution. It should be noted that in polydisperse samples, reported mean diameters are weighted toward larger agglomerate sizes, because the amount of light scattered by larger nanoparticles is greater than that of smaller nanoparticles.

### *Matrix characterization*

Two different matrices were used for the present study: A 50- to 70-mesh white quartz sand (catalog no. 274739, batch 11305KD; Sigma-Aldrich), and soil collected from Okaloosa County (FL, USA). Soil was passed through a 30-mesh sieve and dried before use. Soils were characterized as Lakeland sand, 0 to 5% slopes (Thermic, coated Typic Quartzipsamments), excessively drained, little to no profile development, pH approximately 5.3, and organic matter content of 0.75% [28]. Reported particle size distributions for Lakeland sand are 92.5% sand (particle size, 50–200 μm), 4.5% silt (particle size, 2–50 μm), and 3% clay (particle size, <2 μm) (<http://websoilsurvey.nrcs.usda.gov/>).

### *Soil column setup*

An automated system for evaluating transport used a sand or soil column, a syringe pump to deliver constant flow, and a 70-μl flow cell for ultraviolet–visible light spectrometry under temperature-controlled conditions (25 ± 2°C; ± refers to standard deviation throughout). Soil columns were constructed from a 100-mm Omnifit® (Biochem Fluidics) borosilicate glass liquid chromatography column (bore size, 6.6 mm) and polytetrafluoroethylene plungers. Plungers were fitted with 105-μm polyester mesh (Small Parts) and silicon no. 005 O-rings (Small Parts) to hold soil and sand in the column while al-

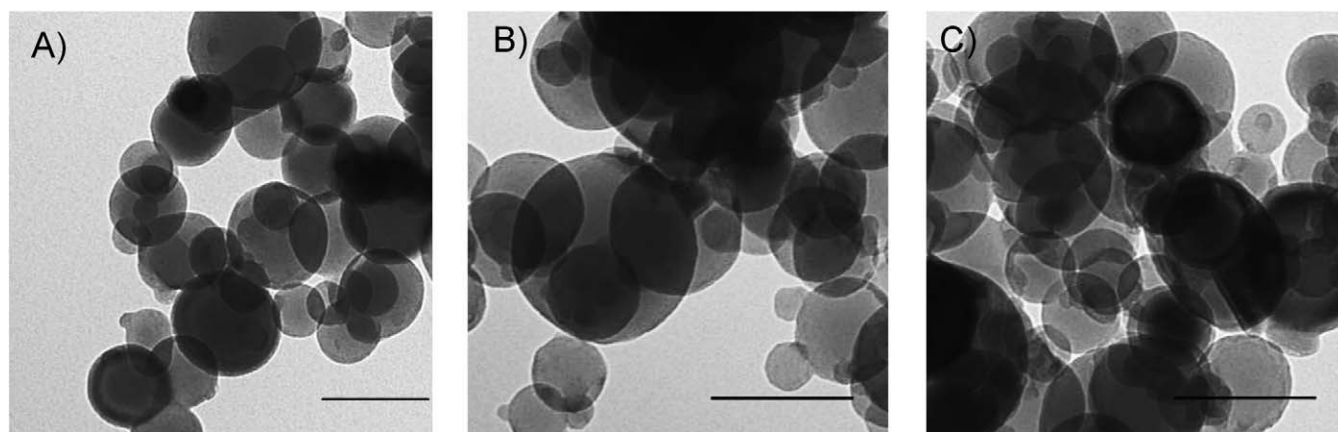


Fig. 1. Transmission-electron microscopy image of (A) 50-nm, (B) 80-nm, and (C) 120-nm aluminum. Nanoparticles were spherical, had broad distribution of sizes, and were agglomerated in the powdered form of the starting material. Bar = 100 nm.

lowing unrestricted flow of nanoparticles. Pore volumes (ml) were calculated as the difference between the total column volume and the matrix volume.

Top-loaded columns were prepared with  $3.88 \pm 0.01$  g of sand. Columns initially were packed with tapping to settle the sand/soil and reduce air spaces. Approximately 7.8 to 8.8 mg of powdered aluminum were layered on top of the sand columns (sand density,  $2.6 \text{ g/cm}^3$ ) for a final column density of  $1.71 \pm 0.01 \text{ g/cm}^3$ . Very soft reconstituted water [27] was passed through the column at a rate of 50 ml/h. Very soft water with low ionic strength and porous sand media was used as a model for maximum transportability under potentially applicable in situ conditions.

Suspension-loaded columns were packed with  $3.87 \pm 0.01$  g of sand or  $3.46 \pm 0.01$  g of soil (soil density,  $2.4 \text{ g/cm}^3$ ), with a final column density of  $1.68 \pm 0.01$  and  $1.60 \pm 0.01 \text{ g/cm}^3$ , respectively. Columns were rinsed repeatedly with solution, and then each column was washed with an additional 100 ml of water or MHRW before loading with aluminum nanoparticles. The aluminum colloidal suspension was introduced by upflow to the column at a constant flow rate of 3 ml/h for 16.7 h (total flow volume, 50 ml) with an automated syringe pump (Braun Perfusor® Compact S). Naturally occurring aluminum in soil did not affect the results of the transport experiments because the concentration of particles transported through the column were monitored as the change in absorbance compared to the final wash eluent. The zeta potential and hydrodynamic diameter of the starting material, ending material, and aliquoted fractions were monitored throughout both experiments using laser Doppler electrophoresis and dynamic light scattering. The absorbance spectrum was measured every 100 s during the course of the experiment. The absorbance at each time point relative to the initial absorbance ( $C_0$ ) at a wavelength of 700 nm was plotted as a function of the volume of nanoparticle solution introduced into the column. The 700-nm wavelength was selected because it monitors aluminum specifically and was minimally affected by other soil matrix particulates eluting from the column.

#### Study area characteristics

Soils from Okaloosa County were selected as highly relevant material for modeling because energetic devices containing aluminum nanoparticles are used routinely in this area. Annual rainfall averages 73 inches, with relatively even distribution throughout the year and occasional flooding. Mean

daily temperatures are between 11 and 27°C. The area of interest is drained by two different stream systems with surface water pH 5.3.

## RESULTS AND DISCUSSION

### Powdered particle characterization

Particle sizes as specified by the manufacturer were 50, 80, and 120 nm and were based on calculations from the Brunauer, Emmett, and Teller specific surface area of 44, 28, and  $18 \text{ m}^2/\text{g}$ , respectively. The geometric mean particle diameter (95% confidence interval) measured by TEM in the present study was 41 (13–128), 52 (17–158), and 74 (25–220) nm. Electron micrographs are presented in Figure 1. We found an 18 to 38% difference in particle diameter, depending on whether it was calculated from specific surface area provided by the manufacturer or measured by TEM. The TEM measurements were used for calculating size distributions based on particle number, surface area, and mass (Fig. 2). Each of these distributions was reported because the most appropriate metric for describing the dose of nanomaterials is still being debated [8,11].

### Suspended particle characterization

Nearly all dry powders of nanoparticles when dispersed in a liquid are in a highly agglomerated state that is dynamic with time; therefore, monitoring nanoparticle agglomerates in suspension and comparing the as-received size with the as-dosed size has been identified as a significant obstacle to interpreting the available literature [11]. Because the formation of agglomerates will increase settling rates in suspension [29] and may impact deposition from a colloidal suspension to a solid surface [30], the agglomeration state and stability of untreated and treated particles in water before introducing them to the columns and at the conclusion of the experiment (16.7 h) are presented in Figure 3A. The hydrodynamic diameter as determined by dynamic light scattering (intensity-weighted Z average  $\pm$  polydispersity index width) of the 50-nm treated aluminum was  $204 \pm 100$  nm at the start of the experiment and was stable throughout the course of the experiment, with an ending diameter of  $204 \pm 101$  nm (16.7 h). The untreated 50-nm aluminum particles diluted in water were similar to the treated particles at the start of the experiment ( $215 \pm 99$  nm); however, the particles agglomerated during the experiment and, by the end, were  $672 \pm 379$  nm. The untreated nominal 80-nm particles were very similar to the 50-nm untreated par-

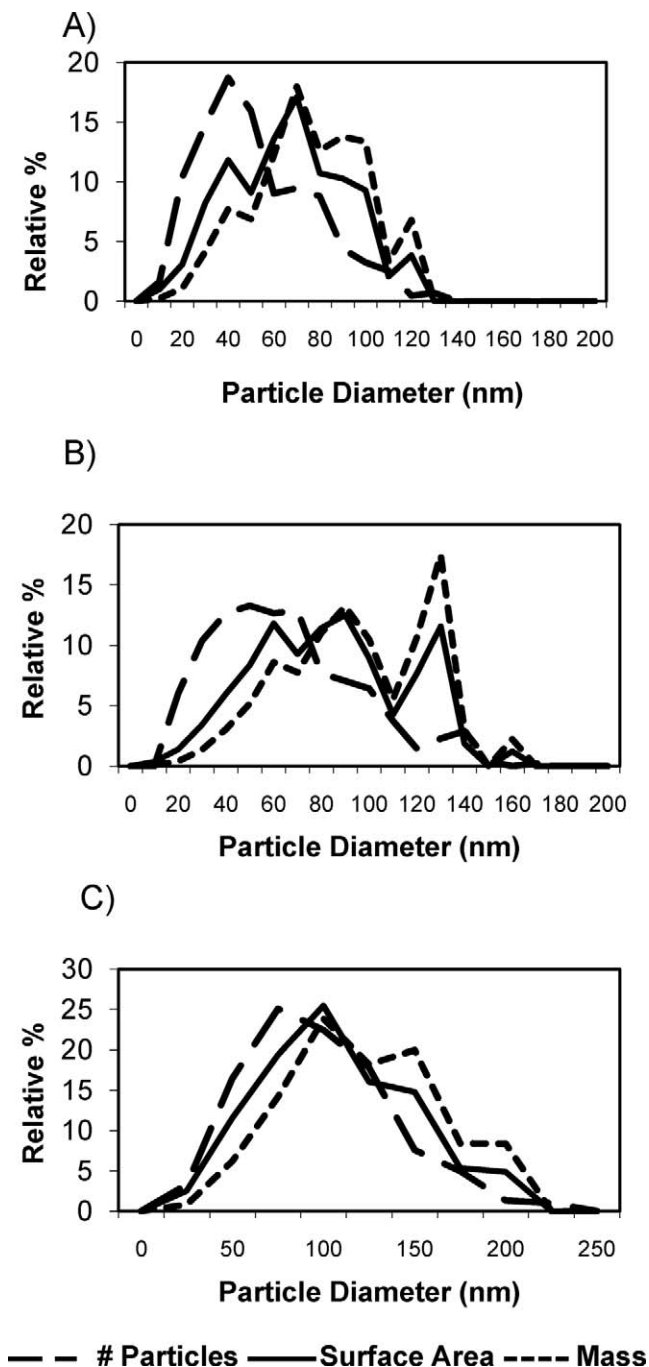


Fig. 2. Particle size distribution histograms based on particle diameter, surface area, and mass for (A) 50-nm, (B) 80-nm, and (C) 120-nm aluminum.

ticles, with diameters of  $210 \pm 95$  nm at the start and  $489 \pm 161$  nm at the end. The 120-nm untreated particles formed larger agglomerates than all other treated or untreated particles in water, with a starting size of  $317 \pm 180$  nm and an ending size of  $1,500 \pm 937$  nm.

Particles treated with phosphate and diluted in water were the most stable over time and had the smallest agglomerate size of the particle/suspension solution combinations evaluated. Phosphate binds strongly to aluminum surfaces, and the phosphate coating on the treated aluminum particles increases the long-term stability of the nanoparticle solution and protects the nanoparticles from oxidation. The effect of the phosphate

coating on the zeta potential of the 50-nm aluminum particles is shown in Figure 3B. Initially, the zeta potential of the untreated 50-, 80-, and 120-nm nanoparticles was strongly positive. In contrast, the zeta potential of the treated particles were strongly negative ( $-40$  mV), indicating that the phosphate had bound to the surface and reversed the charge on the nanoparticle. Over time, the treated particles remained stable in both size and zeta potential, whereas the untreated particles increased in size and had a reduced zeta potential. As demonstrated in the transport experiments presented below, the difference between the surface state of the treated and untreated nanoparticles had a dramatic effect on the transport dynamics of aluminum nanoparticles.

To simulate typical groundwater conditions, the nanoparticle agglomeration state and zeta potential were investigated in MHRW. The starting and ending hydrodynamic diameter of treated and untreated, nominal 50-nm aluminum nanoparticles in water and MHRW are shown in Figure 3C. In both the treated and untreated cases, the higher-ionic-strength MHRW destabilized the aluminum nanoparticles, resulting in an increase in the starting and final hydrodynamic diameters. The 50-nm untreated material diluted in MHRW was the least stable of all aluminum formulations measured, with a starting hydrodynamic diameter of  $791 \pm 400$  nm and a final diameter of  $2,344 \pm 1,997$  nm. Likewise, the 50-nm treated particles diluted in MHRW were larger than their counterparts diluted in water, with a diameter of  $461 \pm 325$  nm at the start and  $1,147 \pm 507$  nm at the end of the experiment. Large agglomerates (particle size,  $>2$   $\mu$ m) precipitated from solution within an hour of suspension. Treated and untreated particles diluted in MHRW formed agglomerates two- to fourfold larger at the start of the experiment and three- to sixfold larger at the end as compared to the particles in water (Fig. 3C). Aluminum nanoparticles agglomerate in cell culture media solutions (F12K supplemented with 20% fetal bovine serum in 1% penicillin and streptomycin) [31] and in phosphate-buffered saline [32], both of which have high ionic strength. Likewise, the present study found that suspension of the aluminum nanoparticles in solutions with higher ionic strength, such as MHRW, caused larger agglomerates in a shorter period of time compared to suspension in water. Ionic strength and a pH near the isoelectric point of the particle have been identified as factors causing agglomeration in solution [12]. The MHRW has both high ionic strength and a pH near the isoelectric point for alumina (pH 7.7), which neutralizes the surface charge of the aluminum nanoparticles and decreases the electrostatic interaction barrier between the particles, allowing agglomerates to form.

The zeta potential of treated and untreated aluminum nanoparticles is shown in Figure 3D. The zeta potential of aluminum particles in water was strongly positive ( $>30$  mV), and the surface charge stayed strongly positive throughout the course of the experiment. In MHRW, however, the starting and final zeta potential measurements were nearly neutral ( $<5$  mV), indicating instability. The neutral zeta potential correlated with the increase in the agglomerate size of the nanoparticles in MHRW. Treated nanoparticles diluted in MHRW began with a negative zeta potential, which was neutralized. The change in charge was not as dramatic as that of the untreated particle, suggesting that the phosphate coating provided some degree of stabilization in MHRW but not enough to completely protect the nanoparticles from agglomerating.

The dramatic changes in the nanoparticle properties with

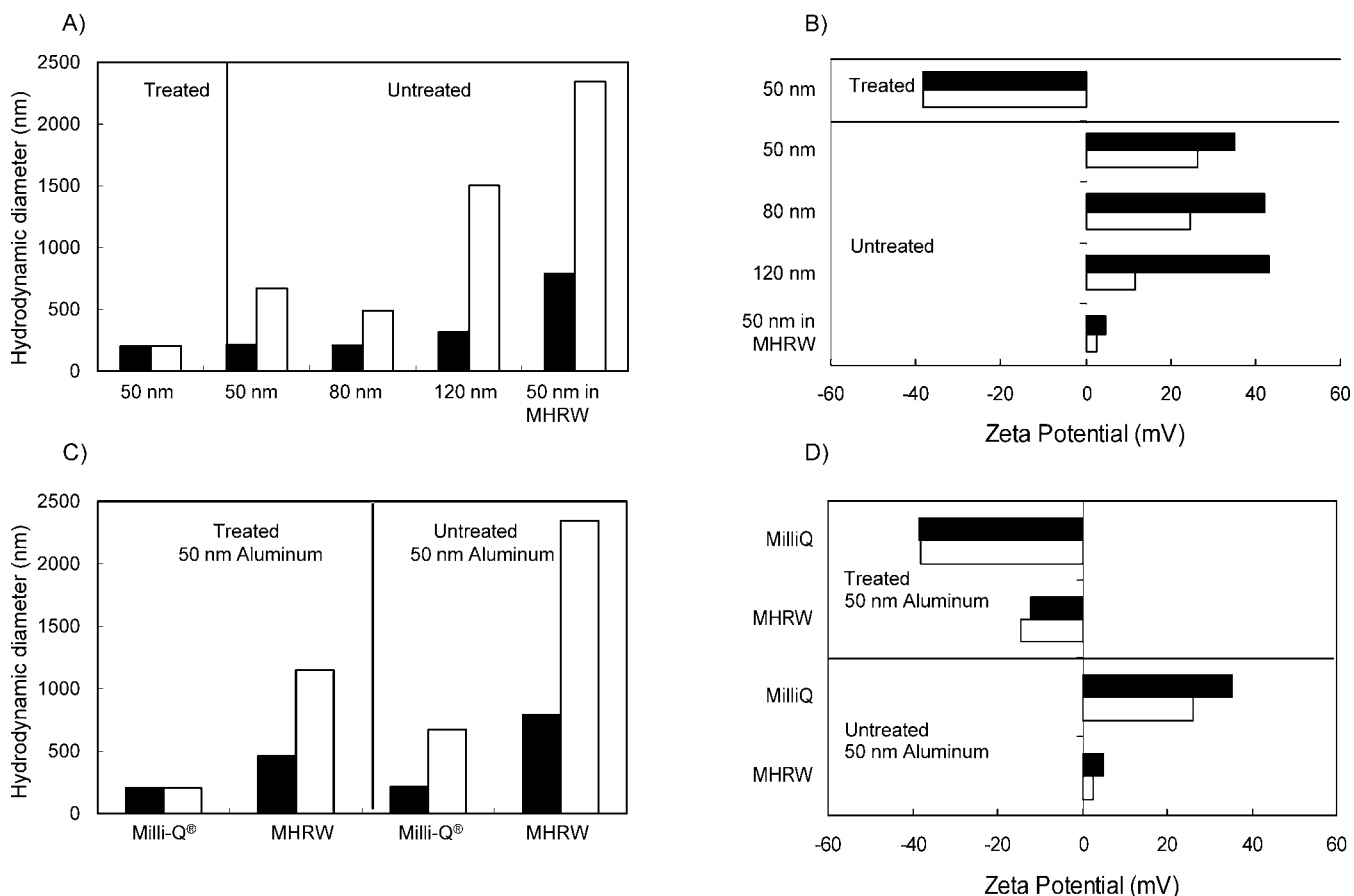


Fig. 3. Agglomerate size and zeta potential of untreated and phosphate-treated (Treated) aluminum nanoparticles in different solutions (Milli-Q® water if not noted or moderately hard reconstituted water [MHRW]) at the start and end of the soil transport experiments. (A) Agglomerate size of aluminum nanoparticles of different primary grain size. (B) Zeta potential of aluminum nanoparticles of different primary grain size. (C) Agglomerate size of treated and untreated aluminum nanoparticles in different solutions. (D) Zeta potential of treated and untreated aluminum nanoparticles in different solutions. Start, 0 h; end, 16.7 h.

introduction to different solutions and treatments demonstrate the potential for diverse interactions with environmental matrices. Surface charge has been shown to be a primary factor in transport through soils [33] and in capture efficiency by filter-feeding organisms [34]. Suspensions of aluminum particles treated with phosphate were negatively charged and the most stable. Moderately hard reconstituted water neutralized the zeta potential of the nanoparticles and accelerated agglomeration. Untreated aluminum nanoparticles had a strong positive charge, which influenced transport through sand and soil matrices. The interactions pertinent to predicting environmental fate and transport and to defining exposure scenarios for ecological risk assessments were explored further, as detailed in the following sections on transport.

#### Transport of aluminum nanoparticles by top-loaded column

Results with 50-nm aluminum nanoparticles in a sand column indicated little risk of transport given the scenario of deposition and infiltration via rainwater. Transport experiments were run in triplicate, and absorbance at breakthrough, defined as the relative maximum concentration compared to the control, ranged from a 0 to 6% increase in absorbance compared to a very soft water-only control. A small amount of material could be observed traveling a short distance through the column, but the leachate was transparent. Doshi et al. [26] evaluated aluminum transport in sand using a similar top-loaded

design by placing 200 mg of 100-nm aluminum on a sand column and eluting with 0.01 M NaCl. Significant clogging of the column prevented passage of the leaching solution, and the experiment was abandoned for another column design in which 80 mg of 100-nm aluminum were placed between sand layers and eluted with 0.01 M NaCl. A spike in the aluminum concentration of the leachate (8 mg/L) at pH 7 was measured after approximately 180 ml of solution passed through the column, but the leachate concentration returned to a value of less than 0.2 mg/L after 240 ml. Unlike the study by Doshi et al. [26], the present study did not measure soluble aluminum in leachate. The ultraviolet–visible light spectrophotometer used in the present study could only detect changes in the leachate absorbance and was not sensitive to soluble aluminum passing through the column. It is possible that some amount of soluble aluminum was passing through the column, as indicated by Doshi et al. [26], but at a circumneutral pH, aluminum solubility is low and transport likely to be minimal. Because of the clogging of the column and negligible transportability, testing was not continued with other particle sizes or matrices and will not be discussed further. The second experimental design using suspension-loaded columns yielded more reproducible results; therefore, the remaining discussion is limited to the suspension-loaded column experiment.

#### Size-related transport in suspension-loaded columns

The transport of the nominal 50-, 80-, and 120-nm powdered aluminum nanoparticle materials was measured in a soil

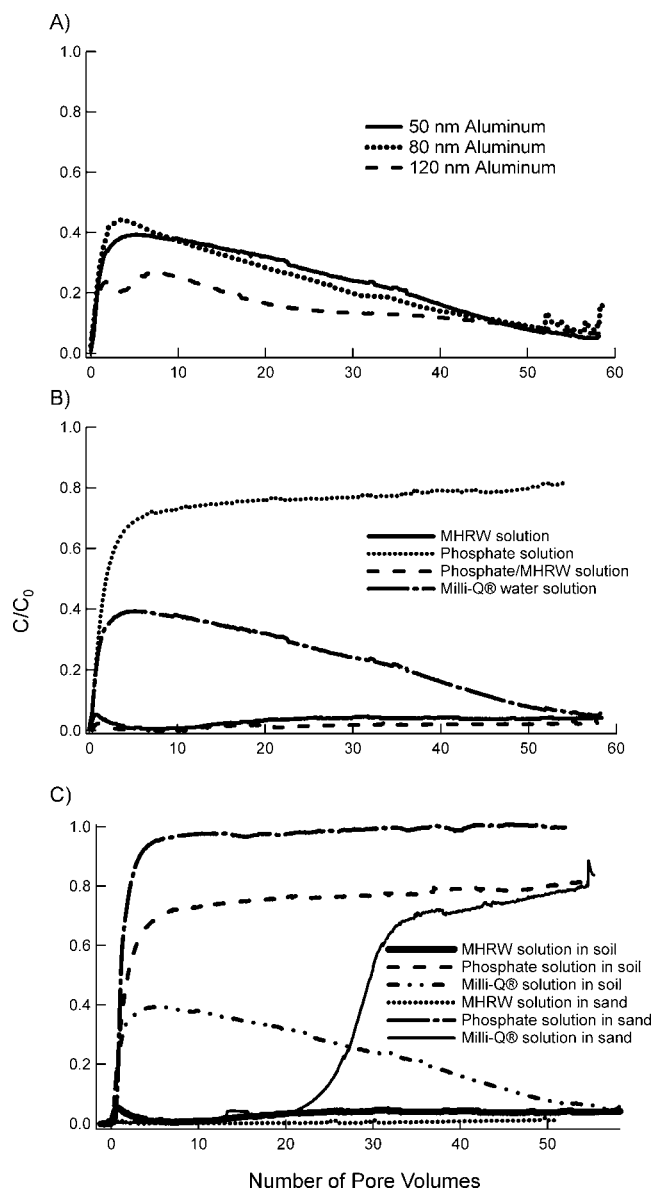


Fig. 4. (A) Size-dependent transport of aluminum nanoparticles through soil based on the change in concentration from the initial ( $C/C_0$ ) measured by absorbance at 700 nm. (B) Transport of 50-nm aluminum nanoparticles suspended in phosphate, moderately hard reconstituted water (MHRW), and Milli-Q® water solutions. (C) Transport of 50-nm aluminum nanoparticles suspended in phosphate, MHRW, and Milli-Q water through two different media (sand and soil).

column. The particles were prepared at a concentration of 50 mg/L in Milli-Q water, sonicated, and immediately loaded to the column. The transport data for the three primary sizes of aluminum are shown in Figure 4A. The concentration at breakthrough was 39 and 44% of  $C_0$  for the 50- and 80-nm particles, respectively, with transport decreasing as the number of pore volumes increased. The transport potentials of 50- and 80-nm aluminum were predicted to be comparable, because the average agglomerate size of each suspension was similar (~210 nm). The 120-nm aluminum nanoparticle had a larger hydrodynamic diameter (317 nm) and, consequently, had a lower concentration at breakthrough, which was attributed to a filtration effect by the matrix grains.

After transport, the mean agglomerate size was two- to

fivefold larger than the starting material, indicating that agglomeration takes place in water for all particle sizes over time. Because the agglomerate size was increasing and the zeta potential decreasing, it was difficult to determine which parameter was leading to the decrease in transport with time. Additionally, even at breakthrough, where the concentration is the highest, approximately 60% of the nanoparticles were still being deposited in the soil column. The accumulation of nanoparticles in the matrix changed the effective pore size of the soil and, potentially, reduced transport. The local dynamics of nanoparticle retention in the column may be complicated by the increase of shear forces created by fluid flow through plugged pores, resulting in partial deagglomeration and mobilization of particles [33]. Further research with nanoparticles that have stable sizes and surface chemistries will be necessary to understand the complicated dynamics of nanoparticle transport in heterogeneous media.

#### Surface charge and solution effects on transport

The impact of dilution media and changes in the surface charge on transport of the nanoparticles was investigated (Fig. 4B). Phosphate treatment was used to mimic release of negatively charged nanoparticles to the environment. Moderately hard reconstituted water was used as a representative dilution media for surface waters, and deionized water served as a control. Phosphate-treated particles in water initially broke through the soil columns at 71% of  $C_0$ , whereas untreated particles in water broke through at 39% of  $C_0$ . After breakthrough, however, transport of the treated particles was between 71 and 82% of  $C_0$  throughout the rest of the experiment, whereas the concentration of the untreated particles dropped dramatically to approximately 5% of  $C_0$ . All particles diluted in MHRW (phosphate treated or not) broke through and remained at less than 6% of  $C_0$ , indicating that regardless of surface treatment, suspension in MHRW reduces transport potential. The primary factors influencing transport were the electrostatic interaction of the particles with soil matrix and the filtration effect of the soil matrix on particles. Both primary size and agglomerate size were important metrics influencing filtration effects, and both mechanisms likely interacted to some degree, but in varying proportions at different size scales, as indicated by the results discussed below.

Both surface charge and agglomeration state have been identified previously as being strongly influential on colloid transport through soils [25,35]. Our transport experiments showed that electrostatic interactions were important, as indicated by the higher rate of transport of the negatively charged, treated particles compared to untreated particles. Derjaguin–Landau and Verway [36,37] theory predicts repulsion between two similar but strongly charged surfaces, such as negatively charged, treated particles and soil. The relative rate of retention of the untreated particles in the column therefore can be explained by the attraction between their positive surface and the predominantly negative surface of the soil particles. Similar interactions were observed in the transport of titania particles in a micromodel system [33]. Oppositely charged particles compared to the matrix surfaces resulted in deposition of the particles in the matrix of the model system, whereas similarly charged matrix and particles resulted in transport of suspended particles through the system.

The electrostatic interaction between matrix and nanoparticle has been described as a critical factor in predicting transport, particularly at the nanoscale [29,33]; therefore, an ex-

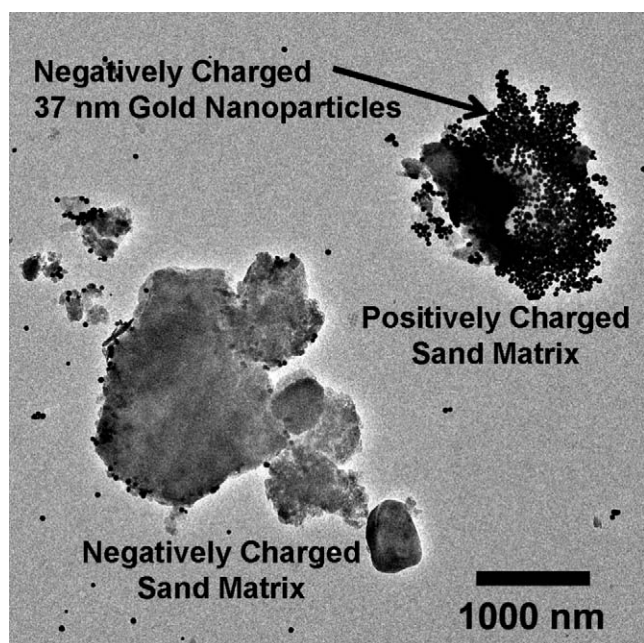


Fig. 5. Negatively charged citrate gold nanoparticles attached to positively charged particulates in soil.

perimental evaluation of the soil matrix and nanoparticle interaction was performed. Although not entirely valid for calculating interaction energies of particles at the nanoscale, classic Derjaguin–Landau and Verwey–Overbeek theory does demonstrate the importance that surface charge has for describing transport under certain conditions [30,33]. This theory states that the interaction of two surfaces in a colloid solution is described by the sum of the van der Waals forces and electrostatic interactions between the surfaces [36,37]. As particle size decreases, van der Waals forces decrease, making the overall interaction of surfaces in aqueous media largely influenced by electrostatic interactions at the nanoscale [29]. To investigate the distribution of charge within a heterogeneous soil sample and the homogenous white quartz sand, gold nanoparticles with different surface charges were used to measure indirectly the surface charge distribution on soil and sand components by assuming that particles of opposite charge will be attracted to each other. Monodisperse, negatively charged, 37-nm gold nanoparticles were passed through the column system, and adsorption to the matrix was imaged using TEM. The sand experiment showed no gold bound to the matrix, indicating that the sand matrix had a homogenous, negative charge, and particles and matrix components with similar charges had minimal electrostatic interaction at the matrix surface. The soil experiment showed very few negatively charged gold particles bound to the soil components, confirming that the soil used in the present study primarily was negatively charged; however, adsorption of gold to a fraction of soil components (comprising ~2% of soil particles) was observable (Fig. 5). It appears that some fraction of the soil had a positive charge and confirmed that localized electrostatic interactions took place within heterogeneous soil matrices with nanoparticles.

Although electrostatic interactions between particles and soil surfaces explained the difference in magnitude of the initial breakthrough between treated and untreated particles of the same size, it did not explain why untreated particles were increasingly retained in the column over the course of the experiment (Fig. 4B). If the interaction between the nanopar-

ticles and soil resulted solely from the electrostatic interactions, then once positively charged aluminum nanoparticles bound to all the negatively charged surfaces in the soil matrix, the transport of the untreated aluminum nanoparticles should have increased. It is hypothesized that the change in agglomerate size with time (from 215 to 672 nm in diameter) was partially responsible for this effect. The larger particles more likely were excluded by the pore size of the matrix, and with larger particles, a greater potential existed for settling before introduction to the column. In contrast, the treated particles had a stable size (204 nm) throughout the experiment, and transport remained constant as a function of the number of pore volumes. In addition to the increase in size, a decrease in the zeta potential of the untreated nanoparticles as a function of time was observed (Fig. 3C), and this may have contributed to the rate at which untreated aluminum nanoparticles were extracted by the matrix. Similar changes in charge density and particle agglomeration have been documented for amphiphilic polyurethane nanoparticles interacting with background electrolytes in soil [38]. This is not surprising, given that high-strength ionic solutions cause agglomeration of nanoparticles [39] by changing the surface charge, which reduces the electrostatic repulsion barrier between particles and amplifies the relative magnitude of van der Waals forces.

#### Transport through different soil types

To investigate further the interactions of aluminum nanoparticle with the matrix, treated and untreated aluminum nanoparticles were transported across white quartz sand. The sand matrix was comprised of a homogenous primary grain size (0.2–0.3 mm), with each grain having a negative surface charge. The investigation of a matrix with a more consistent charge distribution and larger porosity than the soil provided clarity regarding the relative importance of the interactions between the filtration capacity of the matrix and the aluminum nanoparticle surface charge. Data from the transport of treated and untreated aluminum nanoparticles in MHRW, water, and phosphate solution are shown in Figure 4C. For the treated nanoparticles in phosphate, breakthrough in the sand column occurred at five pore volumes, and a concentration of 95% of  $C_0$  indicated that the negatively charged aluminum nanoparticles did not interact with the matrix and were not restricted by pore size. Treated particles with small size and large interaction energy barriers passed through the pore spaces without interacting. Dunphy Guzman et al. [33] suggest that interaction energy barriers and agglomerate size may play key roles in predicting transport. Untreated nanoparticles through sand had a very different profile. Breakthrough with the positively charged nanoparticles was delayed until 27 pore volumes, with an initial transport of 68% of  $C_0$ , presumably caused by binding of the positively charged aluminum nanoparticles to the surface of the sand matrix. After 27 pore volumes, an estimated 1.207 mg of aluminum had been extracted from solution onto the matrix, corresponding to a surface coverage of 18% of the sand matrix, with 213-nm aluminum agglomerates (assuming a 50% agglomerate porosity) binding to the surface of sand grains (particle size, 250  $\mu\text{m}$ ). Because of the spreading dynamics of agglomerates on the surface of substrates and smaller agglomerates covering the surface more efficiently than larger agglomerates, this calculated coverage is what would be expected if breakthrough were caused by a saturation of negatively charged binding sites on the sand particles. Transport of untreated nanoparticles in MHRW showed

impeded transport resulting from destabilization of the aluminum nanoparticles into agglomerates. Even with a much larger pore size as compared to the soil matrix, transport through the sand in MHRW was very low.

If the transport in soil columns described earlier is compared to the experiments with the sand matrix, transport of both treated and untreated aluminum nanoparticles in the soil matrix was less than that in sand. The transport of the treated particles through the sand had breakthrough at five pore volumes and relatively high transport (95% of  $C_0$ ) as compared to a breakthrough in six pore volumes (71% of  $C_0$ ) in the soil column (Fig. 4C). Likewise, although delayed, untreated particles in water were transported more efficiently through the sand column (68% of  $C_0$ ) compared with soil (39% of  $C_0$ ). Untreated particles diluted in MHRW had exceptionally low passage by the sand (<2% of  $C_0$  at breakthrough) and the soil column (6% of  $C_0$ ).

The difference in transport of the particles through sand and soil matrices can be predicted based on electrostatic interactions between the particles and matrix, the dynamic pore size of the matrix over time, and the higher surface area per unit mass of the soil. Electrostatic binding of particles to the matrix contributed to clogging of pore spaces, effectively reducing the pore size of the matrix over time and increasing the effect of filtration [35]. The additive contribution of smaller pore sizes, increased filtration rate, and a larger surface area for electrostatic interactions also explains why transport in soil was less than that in sand. Additionally, because the nanoparticles remain in environmentally relevant solutions, the aggregation size of the particles increased. As the particles became larger throughout the experiment, the effect of filtration became greater, as more and larger particles were impeded by the matrix. Although filtration likely was important throughout the entire column, a collection of untreated aluminum diluted in water in the soil column was observed at the site of introduction; this collection was not observed in the sand column or for the treated particles diluted in water. When untreated particles in water were first introduced to the column, a strong electrostatic effect occurred, and the particles bound to the oppositely charged matrix. Pore sizes therefore were reduced by this binding, which impeded the transport of progressively smaller particle sizes through the column. The effect of filtration in the pore spaces and agglomeration over time may be partially responsible for the magnitude of the reduction in transport through soil—a similar effect has been shown to play a role in other transport studies [33,35]. Because treated particles in water had a small and stable diameter, the pore size had limited impact on physical filtering, and collection of aluminum on introduction to the column was not observed.

## CONCLUSION

The present study demonstrated that the characteristics of nanoparticles are dynamic in the environment and that this is an important consideration for the design and interpretation of nanoparticle studies. The properties of aluminum nanoparticles were monitored in different solutions, and the transport of aluminum nanoparticles was investigated in soil and sand matrices. Although aluminum chemistry is complicated and many factors may be implicated in soil transport processes, certain basic principles are deterministic in predicting transport of aluminum particles in soils at circumneutral pHs, such as size, surface charge, and agglomeration rate. Transport of aluminum nanoparticles was inversely related to the size of the agglom-

erated particles. Depending on the ionic strength of the solution in which they are suspended, the agglomerate size can increase with time and further affect transport. In solutions that mimic surface water conditions of moderate ionic strength, aluminum nanoparticles will rapidly form micron-sized agglomerates and restrict transport. Similarly, particles loaded to the top of the column had limited transport because of clogging of the matrix by agglomerates. Particles that remain unagglomerated and relatively small (~200 nm) have greater transport potential, however, and could potentially reach groundwater or surface water. Additionally, the surface charge of the particles and the receiving matrices also are important, particularly for small, stable agglomerates, where surface charge may be most influential in describing transport. Generally, particles with a surface charge similar to that of the matrix are transported, and those with opposite charges are retained in the matrix. Binding to uncharged elements in the soil will occur, but to a lesser degree than when an electrostatic attraction exists between the particles and soil. As indicated by the results presented here, the surface charges of the particles and the soil may be the dominant physicochemical characteristics governing transport of nanoparticle agglomerates at size ranges not subject to filtration. Predictive models should be developed for nanoparticle transport in different matrices based on relationships between rates of agglomeration, size of the starting material, and charge of the nanoparticle and the matrix. Further work should include evaluation of other nanoparticles in multiple soil types, use of particles that are stable in environmental solutions, comparison of engineered nanoparticles to naturally occurring nanomaterials (e.g., comparing released aluminum nanoparticles to nanoscale gibbsite in the soil), and investigation into other relevant interactions, such as the effect of organic acids on nanoparticle characteristics and transport.

The objective of the present study was to identify how nanoparticles with novel physicochemical properties may interact with the environment, with the goal of specifically designing particles that have limited transport potential. Knowledge regarding the basic principles governing transport also is critical in identifying realistic pathways of exposure to environmental media and biota and in considering how the material should be characterized to design environmentally relevant toxicity studies and risk assessment evaluations. Clearly, salts found in the environment greatly impact aluminum nanoparticles by causing agglomeration and by decreasing transport and, potentially, bioavailability. A number of interactions between the media, carrier solution, and particles in the in vivo model still need to be identified, and even greater interactions likely exist that may impact in situ systems. Further work needs to address how particles interact or bind with specific soil constituents as well as how particles may change with time in different media.

*Acknowledgement*—This work was funded under the U.S. Air Force Small Business Innovation Research Contract FA8651-06-C0136.

## REFERENCES

1. Colvin VL. 2003. The potential environmental impact of engineered nanomaterials. *Nat Biotechnol* 21:1166–1170; Erratum 22: 760.
2. Hoet PHM, Brüske-Hohlfeld I, Salata OV. 2004. Nanoparticles—Known and unknown health risks. *Journal of Nanobiotechnology* 2:12–27.
3. Warheit DB. 2004. Nanoparticles: Health impacts? *Mater Today* 7:32–35.

4. Nel A, Xia T, Madler L, Li N. 2006. Toxic potential of materials at the nanolevel. *Science* 311:622–627.
5. Royal Society and The Royal Academy of Engineering. 2004. Nanoscience and nanotechnologies: Opportunities and uncertainties. Royal Society Policy Document 19/04. Final Report. London, UK.
6. Handy RD, Shaw BJ. 2007. Toxic effects of nanoparticles and nanomaterials: Implications for public health, risk assessment and the public perception of nanotechnology. *Health Risk Soc* 9:125–144.
7. Owen R, Handy R. 2007. Viewpoint: Formulating the problems for environmental risk assessment of nanomaterials. *Environ Sci Technol* 41:5582–5588.
8. Department of Environment, Food and Rural Affairs. 2007. Characterizing the potential risks posed by engineered nanoparticles. A second UK government research report. Defra Publications, London, UK.
9. Oberdorster G, Maynard A, Donaldson K, Castranova V, Fitzpatrick J, Ausman K, Carter J, Karn B, Kreyling W, Lai D, Olin S, Monteiro-Riviere N, Warheit D, Yang H, ILSI Research Foundation/Risk Science Institute Nanomaterial Toxicity Screening Working Group. 2005. Principles for characterizing the potential human health effects from exposure to nanomaterials: Elements of a screening strategy. *Particle and Fibre Toxicology* 2:8–43.
10. Balbus JM, Maynard AD, Colvin VL, Castranova V, Daston GP, Denison RA, Dreher KL, Goering PL, Goldberg AM, Kulinski KM, Monteiro-Riviere NA, Oberdorster G, Omenn GS, Pinkerton KE, Ramos KS, Rest KM, Sass JB, Silbergeld EK, Wong BA. 2007. Meeting Report: Hazard assessment for nanoparticles—Report from an Interdisciplinary Workshop. *Environ Health Perspect* 115:1654–1659.
11. Powers KW, Brown SC, Krishna VB, Wasdo SC, Moudgil BM, Roberts SM. 2006. Research strategies for safety evaluation of nanomaterials. Part VI. Characterization of nanoscale particles for toxicological evaluation. *Toxicol Sci* 90:296–303.
12. Warheit DB, Hoke RA, Finlay C, Donner M, Reed KL, Sayes C. 2007. Development of a base set of toxicity tests using ultrafine TiO<sub>2</sub> particles as a component of nanoparticle risk management. *Toxicol Lett* 171:99–110.
13. Brant J, Lecoanet H, Hotze M, Wiesner M. 2005. Comparison of electrokinetic properties of colloidal fullerenes (*n*-C<sub>60</sub>) formed using two procedures. *Environ Sci Technol* 39:6343–6351.
14. Skebo JE, Grabinski CM, Schrand AM, Schlager JJ, Hussain SM. 2007. Assessment of metal nanoparticle agglomeration, uptake, and interaction using high-illuminating system. *Int J Toxicol* 26:135–141.
15. Hussain SM, Javorina AK, Schrand AM, Duhart HM, Ali SF, Schlager JJ. 2006. The interaction of manganese nanoparticles with PC-12 cells induces dopamine depletion. *Toxicol Sci* 92:456–463.
16. Brant JA, Labille J, Bottero JY, Wiesner MR. 2006. Characterizing the impact of preparation method on fullerene cluster structure and chemistry. *Langmuir* 22:3878–3885.
17. U.S. Air Force Studies Board. 2006. A Review of United States Air Force and Department of Defense Aerospace Propulsion Needs. Committee on Air Force and Department of Defense Aerospace Propulsion Needs, National Research Council of the National Academies. National Academies Press, Washington, DC.
18. Meda L, Marra G, Galfetti L, Severini F, De Luca L. 2007. Nanoaluminum as energetic material for rocket propellants. *Materials Science and Engineering C* 27:1393–1396.
19. Moore MN. 2006. Do nanoparticles present ecotoxicological risks for the health of the aquatic environment? *Environ Int* 32:967–976.
20. Yang L, Watts DJ. 2005. Particle surface characteristics may play an important role in phytotoxicity of alumina nanoparticles. *Toxicol Lett* 158:122–132.
21. Lin D, Xing B. 2007. Phytotoxicity of nanoparticles: Inhibition of seed germination and root growth. *Environ Pollut* 150:243–250.
22. Tong Z, Bischoff M, Nies L, Applegate B, Turco RF. 2007. Impact of fullerene (C<sub>60</sub>) on a soil microbial community. *Environ Sci Technol* 41:2985–2991.
23. Xu S, Liao Q, Saiers JE. 2008. Straining of nonspherical colloids in saturated porous media. *Environ Sci Technol* 42:771–778.
24. Zhang W. 2003. Nanoscale iron particles for environmental remediation: An overview. *Journal of Nanoparticle Research* 5:323–332.
25. Schrick B, Hydutsky BW, Blough JL, Mallouk TE. 2004. Delivery vehicles for zero-valent metal nanoparticles in soil and groundwater. *Chemistry of Materials* 16:2187–2193.
26. Doshi R, Braidia W, Christodoulatos C, Wazne M, O’Conner G. 2008. Nanoaluminum: Transport through sand columns and environmental effects on plants and soil communities. *Environ Res* 106:296–303.
27. U.S. Environmental Protection Agency. 2002. Short-term methods for estimating the chronic toxicity of effluents and receiving waters to freshwater organisms. EPA821/R-02-013, 4th ed. Office of Water, Washington, DC.
28. Natural Resources Conservation Service. 1999. *Soil Taxonomy: A Basic System of Soil Classification for Making and Interpreting Soil Surveys*, 2nd ed. Natural Resources Conservation Service. U.S. Department of Agriculture Handbook. Pittsburg, PA.
29. Brant J, Labille J, Bottero JY, Wiesner MR. 2007. Nanoparticle transport, aggregation, and deposition. In Wiesner MR, Bottero JY, eds, *Environmental Nanotechnology*. McGraw-Hill, New York, NY, USA, pp 231–294.
30. Elimelech M, O’Melia CR. 1990. Effect of particle size on collision efficiency in the position of Brownian particles with electrostatic energy barriers. *Langmuir* 6:1153–1163.
31. Wagner AJ, Bleckmann CA, Murdock RC, Schrand AM, Schlager JJ, Hussain SM. 2007. Cellular interaction of different forms of aluminum nanoparticles in rat alveolar macrophages. *J Phys Chem B* 111:7353–7359.
32. Braydich-Stolle L, Hussain S, Schlager JJ, Hofmann MC. 2005. In vitro cytotoxicity of nanoparticles in mammalian germline stem cells. *Toxicol Sci* 88:412–419.
33. Dunphy Guzman KA, Finnigan MP, Banfield JF. 2006. Influence of surface potential on aggregation and transport of titania nanoparticles. *Environ Sci Technol* 40:7688–7693.
34. Gerritsen J, Porter KG. 1982. The role of surface charge on filter feeding of zooplankton. *Science* 216:1225–1227.
35. Nyer EK, Vance DB. 2001. Treatment technology: Nanoscale iron for dehalogenation. *Ground Water Monit Remediation* 21:41–46.
36. Derjaguin BV, Landau LD. 1941. Theory of the stability of strongly charged lyophobic sols and the adhesion of strongly charged particles in solutions of electrolytes. *Acta Physico-Chimica Sinica* 14:633–662.
37. Verwey EJW, Overbeek JT, Nes K. 1948. *Theory of the Stability of Lyophobic Colloids: The Interaction of Sol Particles Having an Electric Double Layer*. Elsevier, New York, NY, USA.
38. Tungittiplakorn W, Lion LW, Cohen C, Kim JY. 2004. Engineered polymeric nanoparticles for soil remediation. *Environ Sci Technol* 38:1605–1610.
39. Lead JR, Wilkinson KJ. 2006. Aquatic colloids and nanoparticles: Current knowledge and future trends. *Environ Chem* 3:159–171.